

Au/Fe₂O₃ Water-Gas Shift Catalyst Prepared by Modified Deposition-Precipitation Method

LI Jinwei, ZHAN Yingying, ZHANG Fengli, LIN Xingyi, ZHENG Qi*

National Engineering Research Center of Chemical Fertilizer Catalyst, Fuzhou University, Fuzhou 350002, Fujian, China

Abstract: The Au/Fe₂O₃ catalyst was prepared by co-precipitation, deposition-precipitation, and modified deposition-precipitation methods and was characterized by X-ray diffraction, X-ray photoelectron spectroscopy, and transmission electron microscopy. The catalyst activity for the water-gas shift (WGS) reaction was discussed. Under strictly controlled conditions, the Au/Fe₂O₃ catalyst prepared by modified deposition-precipitation displayed higher activity for the WGS reaction than that prepared by co-precipitation and deposition-precipitation. In the former case, the CO conversion of 82.3% was obtained with a feed gas of 10% CO/N₂ at 150 °C. Wherein, gold particles of 3–5 nm were highly dispersed on the surface of the Fe₂O₃ support that existed in an amorphous and crystalline state. A relatively strong interaction between gold particles and the support occurred, which was beneficial for the WGS reaction.

Key words: modified deposition-precipitation; iron oxide; supported gold catalyst; water-gas shift reaction

The water-gas shift (WGS) reaction has captured the continuous interests of scientists owing to its extensive applications in the treatment of automobile exhaust gas and the purification of hydrogen-rich reformed gas in car-mounted fuel cells. Since Andreeva et al. [1] first reported the high catalytic activity of Au/Fe₂O₃ for the WGS reaction, extensive studies have been carried out on the preparation and microstructure of gold catalysts. The previous studies indicated that the catalytic activity of gold catalysts depends seriously on the preparation process; in other words, different particle sizes can be obtained using various preparation methods, and consequently, various interactions between gold and supports can be observed, leading to disparate catalytic activity [2]. So far, the common methods for preparing supported gold catalysts include impregnation [3], co-precipitation [4], deposition-precipitation [5], and microemulsion methods [6]. Although gold catalysts with good initial catalytic activity can be prepared by these methods under the strict control of experimental conditions in the laboratory, there are many aspects in the preparation process that need to be optimized for industrial applications. In view of this, Andreeva et al. [7] improved the deposition-precipitation method, by which a nano-Au catalyst with high catalytic activity was obtained. Their results indicated that

most of the Au particles dispersed highly on the support surface and the interaction between gold and support was ameliorated. However, Wang et al. [8] and Hua et al. [9] could not reproduce the result when using the same preparation method.

In this study, based on our previous work [9], we prepared the Au/Fe₂O₃ catalysts with high catalytic activity using a modified deposition-precipitation method, and the catalysts were characterized by X-ray diffraction (XRD), X-ray photoelectron spectroscopy (XPS), and transmission electron microscopy (TEM). The effects of the synthesis methods (co-precipitation, deposition-precipitation, and modified deposition-precipitation) on their structures and catalytic activity were also discussed. The relationship between the phase structure of the support and the interaction between gold and the support was investigated.

1 Experimental

1.1 Catalyst preparation

1.1.1 Co-precipitation (CP)

The aqueous solutions of 0.2 mol/L HAuCl₄ and 1.0 mol/L

Received date: 14 September 2007.

* Corresponding author. Tel: +86-591-83731234-8112; E-mail: zhengqi@fzu.edu.cn

Foundation item: Supported by the National Natural Science Foundation of China (20771025) and the Science and Technology Program Foundation of Fujian Province (2002H026).

Copyright © 2008, Dalian Institute of Chemical Physics, Chinese Academy of Sciences. Published by Elsevier BV. All rights reserved.

Fe(NO₃)₃ were mixed under vigorous stirring, the Au/Fe atomic ratio being 1/60. Then, the aqueous mixture was co-precipitated with an aqueous solution of K₂CO₃ (1.0 mol/L) under vigorous stirring. The co-precipitation conditions were as follows: temperature, 60 °C; stirrer speed, 250 r/min; reactant feed flow rate, 6 ml/min; pH = 8.0. After 1 h of aging at 60 °C, the precipitate was alternatively centrifuged and washed with deionized water until no Cl⁻ ions were detected with AgNO₃ solution. The samples were then dried at 120 °C for 8 h and calcined at 300 °C for 2 h in air. The final sample was labeled Au/Fe₂O₃-CP.

1.1.2 Deposition-precipitation (DP)

The support of Fe₂O₃ was prepared from the aqueous solution of Fe(NO₃)₃·9H₂O and K₂CO₃ by the CP method. The support was crushed into fine particles and thoroughly suspended in 50 ml deionized water under ultrasound irradiation. Then, a desired amount of HAuCl₄ was added dropwise into the aqueous slurry of prepared Fe₂O₃ at 60 °C and pH = 8.0. The resulting precipitate was aged at the same temperature for 1 h and then washed with deionized water until there were no residual Cl⁻ ions. Then, the precipitate was dried and calcined in air. The controlled conditions were the same as the CP method, and the final sample was labeled Au/Fe₂O₃-DP.

1.1.3 Modified deposition-precipitation (MDP)

The aqueous solutions of 1.0 mol/L Fe(NO₃)₃ and 1.0 mol/L K₂CO₃ were simultaneously added to 20 ml deionized water at 60 °C and at a constant pH of 8.0 under vigorous stirring. After being centrifuged and washed with deionized water several times, the precipitate was re-dispersed into 50 ml deionized water at 60 °C. Then, a 0.2 mol/L HAuCl₄ solution was pumped into the support slurry prepared under vigorous stirring, maintaining a constant pH of 8.0 by adding 1.0 mol/L K₂CO₃. After an additional 1 h of stirring, the precipitate was alternatively centrifuged and washed with deionized water until no Cl⁻ ion was detected. Then, the samples were dried at 120 °C for 8 h and calcined at 300 °C for 2 h in air. The final sample was labeled Au/Fe₂O₃-MDP.

1.2 Activity measurements

The catalytic activity of the samples for the WGS reaction was measured using a CO-CMAT 9001 apparatus (Beijing Hangdun, China) at atmospheric pressure. The sample charged each time was 0.5 ml (20–40 mesh size) and was preliminarily reduced at 150 °C for 9 h in 10% H₂/N₂ mixture. The mixed gas of 10% CO/N₂ was passed through a vaporizer (at 82 °C) and then was fed into the reactor. The flow rate was 83 ml/min (space velocity = 10000 h⁻¹). Catalysts were tested in the range

of 150–300 °C with a step size of 50 °C. At each test point, the reaction temperature remained unchanged for 6 h. The product gas was directed through a condenser and sent to an online gas chromatograph (Shimadzu GC-8A), where the CO content was analyzed. The catalytic activity is expressed by the conversion of CO, which is defined as $X(\text{CO}) = 100\% \times (1 - V_o/V_i)/(1 + V_o)$, where V_i and V_o are the inlet and outlet contents of CO, respectively.

1.3 Catalyst characterization

The textures of the samples were measured by nitrogen adsorption-desorption isotherms at liquid nitrogen temperature using an OMINSORP 100CX instrument. Prior to analysis, the samples were degassed at 200 °C to 1 mPa.

Powder XRD data of the samples were collected on a PANalytical X'pert Pro diffractometer with an X'Celerator detector using Co K_α radiation ($\lambda = 0.17902$ nm) at a voltage of 40 kV and a current of 20 mA. Diffraction patterns were recorded at room temperature (RT) in a step scanning mode with a 0.0333° (2θ) step size and 40 s/step counting time in the range $20^\circ \leq 2\theta \leq 80^\circ$.

The morphology and microstructure of the samples were characterized using a Tecnai G2 F20 transmission electron microscope (accelerating voltage, 200 kV). Samples for the TEM study were prepared by gently grinding catalyst powder in a mortar followed by ultrasonically dispersing powder in ethanol. The solution was deposited onto a carbon-coated Cu mesh grid via a pipette and then was allowed to dry under ambient conditions.

XPS measurements were performed on a Phi Quantum 2000 spectrophotometer with Al K_α radiation (1486.6 eV). The pressure in the test chamber was maintained below 1.33×10^{-9} Pa during the collection. An electron takeoff angle of 45° was used. The spectra were collected with an analyzer using the pass energy of 46.5 eV. The binding energies were corrected for surface charging by referencing them to the energy of C 1s peak of contaminant carbon at 284.8 eV.

2 Results and discussion

2.1 Catalytic activity

CO conversion via the WGS reaction over the Au/Fe₂O₃ catalysts prepared by different methods as a function of reaction temperature is presented in Fig. 1. The sample prepared by MDP displays high low-temperature WGS activity with 82.3% CO conversion at 150 °C. The catalyst prepared by DP shows the lowest activity, and the CO conversion is only 55% even at 200 °C.

2.2 Nitrogen physisorption

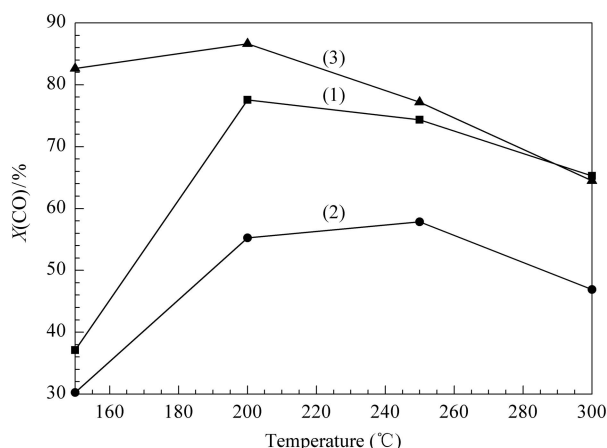


Fig. 1. Effect of preparation methods on the catalytic activity of Au/Fe₂O₃ for WGS reaction. (1) Au/Fe₂O₃-CP; (2) Au/Fe₂O₃-DP; (3) Au/Fe₂O₃-MDP. Catalyst reduction with 10% H₂/N₂ at 150 °C for 15 h preceded all activity tests. CP: co-precipitation; DP: deposition-precipitation; MDP: modified deposition-precipitation.

Table 1 Texture data of Au/Fe₂O₃ catalysts prepared by different methods

Catalyst	BET surface area* (m ² /g)	Pore volume (cm ³ /g)	Average pore radius (nm)
Au/Fe ₂ O ₃ -CP	116 (22)	0.2317	4.0
Au/Fe ₂ O ₃ -DP	79 (16)	0.1174	3.0
Au/Fe ₂ O ₃ -MDP	132 (23)	0.2226	3.4

*The numbers in parentheses denote the BET surface areas of the used catalysts.

The surface area, pore volume, and average pore radius of the samples prepared by different methods are summarized in Table 1. It is observed that the textural properties of the supported gold catalysts are influenced by the preparation method. The average pore radius of all samples is 3–4 nm, but Au/Fe₂O₃-MDP and Au/Fe₂O₃-CP show higher values in both the surface area and pore volume than Au/Fe₂O₃-DP. The surface area of all samples decreases remarkably after reaction, indicating that the structure of catalysts has changed during the pretreatment and the catalytic process [1].

2.3 XRD

The XRD patterns of all samples reduced with 10% H₂/N₂ and after the WGS reaction are shown in Fig. 2. The reduced samples exhibit several peaks related to magnetite and metallic gold, and no peaks of Au₂O or Au₂O₃ are observed. Although the supports in all samples are transformed to magnetite, the intensity of their peaks is different with the preparation method, indicating that the degree of crystallinity of the support varies with the preparation method. The average grain

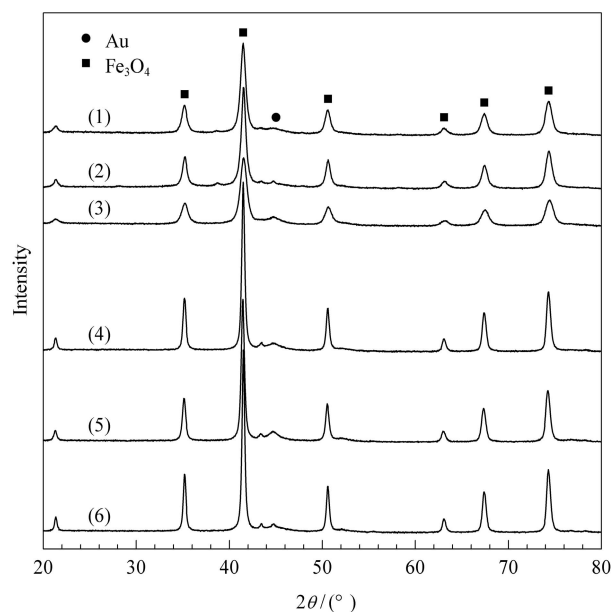


Fig. 2. XRD patterns of Au/Fe₂O₃ catalysts after being reduced and WGS reaction. (1) Au/Fe₂O₃-CP reduced; (2) Au/Fe₂O₃-DP reduced; (3) Au/Fe₂O₃-MDP reduced; (4) Au/Fe₂O₃-CP used; (5) Au/Fe₂O₃-DP used; (6) Au/Fe₂O₃-MDP used.

sizes of the support of Au/Fe₂O₃-CP, Au/Fe₂O₃-DP, and Au/Fe₂O₃-MDP estimated from the line-width of magnetite (74.5°) reflection peak using the Scherrer equation are 22.0, 24.0, and 20.6 nm, respectively. The catalysts that experienced activity tests were also characterized by XRD. It is found that the intensity of the characteristic diffraction peaks of Au(111) increases significantly, the characteristic peaks of magnetite sharpen, and the average grain sizes of the corresponding supports are 45.2, 48.0, and 38.2 nm, respectively. This indicates that serious sintering of gold particles and support particles occurred during the catalytic operation.

2.4 TEM

Fig. 3 shows the bright-field TEM images of Au/Fe₂O₃ catalysts prepared by different methods. As seen in the TEM images, the size of gold particles and the morphology of supports are different owing to the different preparation methods. For the sample prepared by co-precipitation, a relatively non-uniform distribution of gold particle size and gold clusters are observed, and the support exists as an amorphous phase. Andreeva et al. [7] reported that co-precipitation favors the formation of gold clusters and the incorporation of gold into the bulk of the precursor, becoming inaccessible to catalysis.

The image of the sample prepared by deposition-precipitation shows occasional Au particles of ca. 6–8 nm in diameter, distributing on the well crystallized support that possesses observable lattice fringe of Fe₂O₃. One possible explanation for

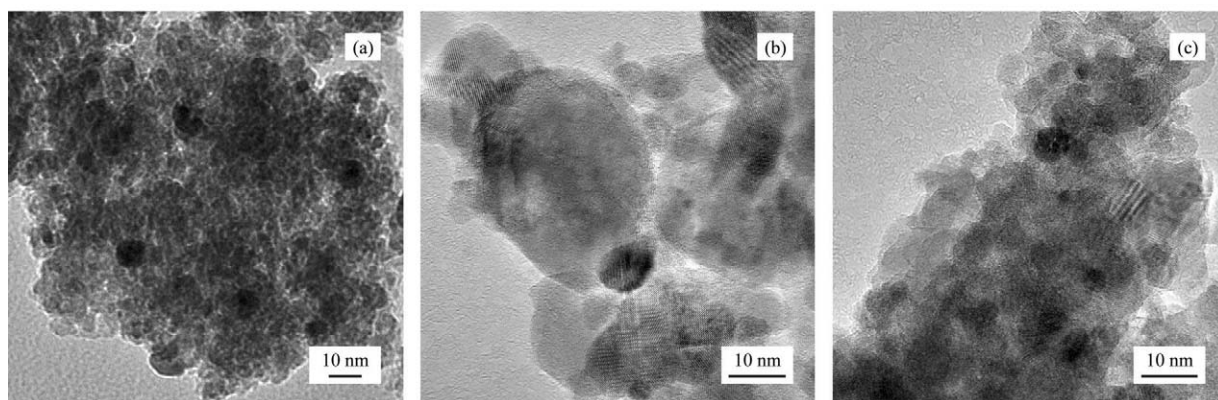


Fig. 3. TEM images of Au/Fe₂O₃ prepared by different methods. (a) Au/Fe₂O₃-CP; (b) Au/Fe₂O₃-DP; (c) Au/Fe₂O₃-MDP.

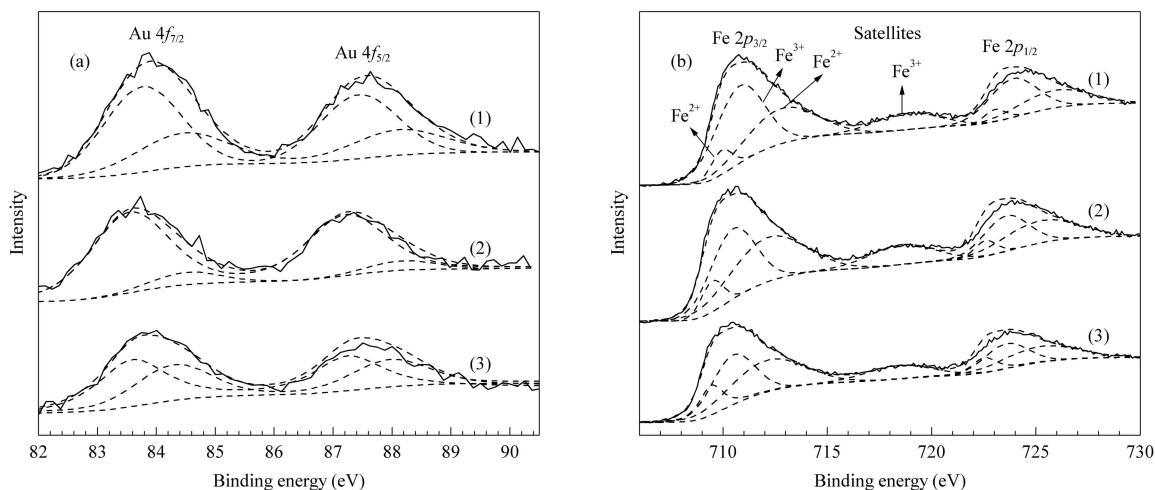


Fig. 4. XPS spectra at Au 4*f* (a) and Fe 2*p* (b) regions of different Au/Fe₂O₃ samples. (1) Au/Fe₂O₃-CP; (2) Au/Fe₂O₃-DP; (3) Au/Fe₂O₃-MDP.

this phenomenon is the twice calcination of support during the synthesis process. As seen in Fig. 3(c), the lattice fringe of Fe₂O₃ is occasionally observed, which indicates that the support of Au/Fe₂O₃-MDP consists of amorphous and crystallized iron oxides. Au particles in all samples are well isolated and highly dispersed on the supports, and the average size is 3–5 nm.

2.5 XPS

XPS was employed to obtain information on the state of gold and iron in the Au/Fe₂O₃ samples prepared by different methods. The results were fitted by a fitting program using a properly weighted sum of Lorentzian and Gaussian component curves after Shirley background subtraction shown in Fig. 4. In detail, the Au 4*f* core level spectra of the Au/Fe₂O₃ are shown in Fig. 4(a). According to the literature [10], XPS peaks of metallic Au (Au⁰) appear mainly at 83.8 eV (Au 4*f*_{7/2}) and 87.45 eV (Au 4*f*_{5/2}). Comparably, those of Au 4*f*_{7/2} in Au⁺

(AuCl) and Au³⁺ (HAuCl₄) can be observed at 86.2 and 87.3 eV, respectively. In our case as shown in Fig. 4(a), all peaks are the characteristic peaks of metallic Au, indicating that gold species have transformed to metallic Au after calcination at 300 °C. Further analyzing the spectrum, Au⁰ was detected with two broad intense bands, one at 83.0–85.0 eV for Au 4*f*_{7/2} and the other at 87.0–89.0 eV for Au 4*f*_{5/2}. The band of Au 4*f*_{7/2} can be fitted into two peaks featuring higher and lower binding energy than 84.0 eV, which should be assigned to the characteristic peaks of Au 4*f*_{7/2} with smaller size gold particles (*d* ≤ 2 nm) and larger size particles, respectively [11,12]. In addition, the ratios of the areas of these two peaks for the as-prepared catalysts are 0.46, 0.12, and 0.49, respectively (Table 2), suggesting that the sample prepared by the deposition-precipitation method has a small percentage of Au particles less than 2 nm.

The electronic configuration of Au is [Xe]4*f*¹⁴5*d*¹⁰6*s*¹ with *d* orbitals being fully occupied; therefore, generally speaking, it has no catalytic activity. However, when Au appears as

Table 2 XPS data for Au/Fe₂O₃ prepared by different methods

Catalyst	Binding energy (eV)							
	Au 4f _{7/2}		Sn1/Sn2*	Fe 2p _{3/2}			Fe ²⁺ /Fe ³⁺	
Au/Fe ₂ O ₃ -CP	83.7	84.5	0.46	709.4	710.6	712.4	718.7	0.239
Au/Fe ₂ O ₃ -DP	83.6	84.5	0.12	709.5	710.5	712.1	718.6	0.192
Au/Fe ₂ O ₃ -MDP	83.6	84.4	0.49	709.4	710.5	712.1	718.4	0.415

* Sn1/Sn2 is the area ratio of the two peaks featuring binding energies higher and lower than 84.0 eV, respectively.

nanoparticles and exhibits non-metallic character, part of Au 5d electrons can transfer into the 3d orbitals of Fe, leading to a positive nature of Au. In this case, d orbitals of Au are partly occupied and exhibit similar electronic structure to that of Pt. Naturally, we can speculate that it will display similar catalytic activity to that of Pt [13]. As revealed by Fig. 4(b), the electronic binding energy of Fe 2p_{3/2} is lowered, compared with the standard spectrum, illustrating an obvious interaction between Au and Fe₂O₃. Besides, the characteristic peaks of Fe 2p_{3/2} can be fitted into two peaks at 709.5 and 710.5 eV, which can be attributed to the peaks of Fe²⁺ and Fe³⁺, respectively. Furthermore, the Fe²⁺/Fe³⁺ ratios in the three samples are different with values being 0.239, 0.192, and 0.415 (Table 2). The difference in valence of surface Fe suggests the different degree of interaction between Au and Fe₂O₃ in the different preparation methods. Taking the previous activity test results into account, it can be concluded that a relatively strong interaction between Au and Fe₂O₃ can be obtained by the modified deposition-precipitation method, which leads to the highest catalytic activity. In addition, binding energy at 712.6 and 718.5 eV may be assigned to high-spin Fe²⁺ 2p_{3/2} and Fe³⁺ 2p_{3/2} shake-up satellite structures caused by Fe 3d-O 2p hybridization [14–16].

3 Conclusions

Different preparation methods lead to the different microstructures and performance of the Au/Fe₂O₃ catalyst, and thus the disparate catalytic activity. The catalyst activity decreases with increasing particle size of iron oxides. The sample prepared by co-precipitation shows nonuniform distribution of gold particle size, and gold clusters are formed during the preparation process. Comparatively, the sample prepared by deposition-precipitation has larger gold particles and higher crystallinity of support. The sample prepared by modified deposition-precipitation has small gold particles and uniform particle size distribution, and its support exists in an amorphous and crystalline state. Gold species are transformed to metallic Au after calcination, which has obvious interaction with the support. Distinct surface Fe²⁺/Fe³⁺ ratio can be explained by the different degree of interaction between gold and the support in the as-prepared catalysts. The crystallinity of the support af-

fects the degree of interaction between gold and the support and has ultimately important effect on the catalytic activity. Thus, the catalyst prepared by modified deposition-precipitation, in which amorphous and crystallized iron oxides are coexistence, has high surface area and small gold particles with uniform distribution and possesses a relatively strong interaction between gold particles and the support, leading to the highest catalytic activity for the WGS reaction.

References

- [1] Andreeva D, Idakiev V, Tabakova T, Andreev A, Giovanoli R. *Appl Catal A*, 1996, **134**(2): 275
- [2] Wang D H, Hao Zh P, Cheng D Y, Shi X Ch. *Prog Natur Sci*, 2002, **14**(8): 794
- [3] Liu Z M, Vannice M A. *Catal Lett*, 1997, **43**(1–2): 51
- [4] Haruta M, Yamada N, Kobayashi T, Lijima S. *J Catal*, 1989, **115**(2): 301
- [5] Tabakova T, Idakiev V, Andreeva D, Mitov I. *Appl Catal A*, 2000, **202**(1): 91
- [6] Chen W, Xiao Y H, Zhan Y Y, Cai G H, Lin X Y, Wei K M, Zheng Q. *Chin J Catal*, 2003, **24**(11): 867
- [7] Andreeva D, Tabakova T, Idakiev V, Christov P, Giovanoli R. *Appl Catal A*, 1998, **169**(1): 9
- [8] Wang G Y, Yu J Y, Lian H L, Li X M, Jia M J, Zhang W X, Wu T H, Ge Y D. *Chem J Chin Univ*, 2000, **21**(5): 752
- [9] Hua J M, Zheng Q, Lin X Y, Wei K M. *Chin J Catal*, 2003, **24**(12): 957
- [10] Moulder J F, Stickle W F, Sobol P E, Bowman K D. *Handbook of X-Ray Photo-electron Spectroscopy*. Eden Prairie, Minnesota: Physical Electronics Inc, 1995. 182
- [11] Rao C N R, Vijaykrishnan V, Aiyer H N, Kulkarni G U, Subbanna G N. *J Phys Chem*, 1993, **97**(43): 11157
- [12] Wang C-T, Ro S-H. *J Non-Cryst Solids*, 2006, **352**(1): 35
- [13] Hao Zh P, An L D, Wang H L, Hu T D. *React Kinet Catal Lett*, 2000, **70**(1): 153
- [14] Weckhuysen B M, Wang D J, Rosynek M P, Lunsford J H. *J Catal*, 1998, **175**(2): 347
- [15] Lin T C, Seshadri G, Kelber J A. *Appl Surf Sci*, 1997, **119**(1–2): 83
- [16] Fujii T, de Groot F M F, Sawatzky G A, Voogt F C, Hibma T, Okada K. *Phys Rev B*, 1999, **59**(4): 3195